JOURNAL OF THERMOPHYSICS AND HEAT TRANSFER
Vol. 21, No. 3, July–September 2007

Technical Notes

TECHNICAL NOTES are short manuscripts describing new developments or important results of a preliminary nature. These Notes should not exceed 2500 words (where a figure or table counts as 200 words). Following informal review by the Editors, they may be published within a few months of the date of receipt. Style requirements are the same as for regular contributions (see inside back cover).

Matching Flight Conditions on Sharp Leading Edges in Plasma Wind Tunnels

Rodolfo Monti,* Raffaele Savino,† and
Mario De Stefano Fumo‡
University of Naples "Federico II," 80125 Naples, Italy

DOI: 10.2514/1.26465

Nomenclature

c_i	=	mass fraction of ith specie
c_p	=	specific heat, J/kg · K
D_i	=	diffusion coefficient of ith specie, m^2/s
Da	=	Damkoeler number
H	=	specific total enthalpy, J/kg
h_{ch}	=	specific chemical enthalpy, J/kg
h_w	=	specific wall enthalpy, J/kg
M	=	Mach number
P_0	=	total pressure, Pa
p	=	pressure, Pa
p_{02}	=	stagnation point pressure, Pa
$\dot{q}_0$	=	stagnation point heat flux, W/m^2
Re_1	=	Reynolds number per unit length, m^{-1}
r	=	curvature radius, m
T	=	temperature, K
V	=	velocity, m/s
Z	=	altitude, km
$(\Delta h_f)_i^0$	=	formation enthalpy of ith specie, J/kg
Δ	=	standoff distance, m
ε	=	emissivity
γ	=	specific heat ratio
λ	=	thermal conductivity, W/m · K
ρ	=	density, kg/m^3
σ	=	Stephan–Boltzmann constant, $W/m^2 \cdot K^4$

Subscripts

t	=	wind tunnel conditions
∞	=	freestream conditions

Introduction

A NEW philosophy of atmospheric reentry has recently been proposed considering a very long trajectory for a low wing loading and high aerodynamic efficiency vehicle that decelerates at higher altitudes than existing reentry vehicles (e.g., shuttle, capsules) [1].

Using new classes of ultrahigh temperature ceramics (UHTC) and the attainment of a sustainable and extremely high radiative equilibrium temperature [2] make it possible to use relatively sharp edges and to achieve the high aerodynamic efficiency necessary to follow high altitude trajectories.

When attempting to simulate free-flight aerothermodynamic conditions in a wind tunnel (e.g., plasma wind tunnel, PWT) because a complete duplication of all relevant flight conditions cannot be achieved (e.g., model scale, p_∞, V_∞ chemical conditions), a finite number of parameters must be selected to simulate aerodynamic heating. In the present context, the convective heat flux distributions over the body surface would be reproduced with particular reference to the stagnation point.

Let us give the guidelines necessary to identify the most appropriate wind tunnel settings simulating free-flight conditions. In a very first approximation, engineering formulas can be used for heat flux at $\dot{q}_0$ as a function of r, of H_∞, of p_{02}, and of h_w. One of the most widely used formulas (Zoby [3]) reads, in international units:

$$\dot{q}_0 = 3.55 \times 10^{-4} \sqrt{\frac{p_{02}}{r}} (H_\infty - h_w) \tag{1}$$

Equation (1) provides the value of stagnation point heat flux for total enthalpy flow up to 10^2 MJ/kg and for a fully catalytic surface.

At hypersonic speeds p_{02} can be approximated by

$$p_{02} \approx \rho_\infty V_\infty^2 \tag{2}$$

Suppose that a hypersonic wind tunnel were able to reproduce p_{02}, H_∞, air composition , and full scale, then the value of $\dot{q}_0$ would be easily duplicated in the wind tunnel: this is seldom the case, however. Typically V_∞ in the tunnel test section, even in the test chamber of the most powerful wind tunnel (e.g., the CIRA Scirocco PWT [4]) is somehow limited to $V_{\infty t} \approx 6000$ m/s.

The p_{02}, in turn, can be reproduced with different values of ρ_∞ and V_∞ (it is necessary to ensure the value of the product $\rho_\infty \times V_\infty^2$). If conditions at velocities exceeding 6000 m/s are to be duplicated, then values exceeding asymptotic density in the wind tunnel test chamber must be selected ($\rho_{\infty t} > \rho_\infty$). Usually there will be a degree of freedom in choosing $\rho_{\infty t}$ (or $V_{\infty t}$); the criteria for the most appropriate choice are discussed below.

The most important difference between free-flight and PWT wind tunnel conditions is that in the latter case total enthalpy $(H_\infty)_t$ includes the kinetic energy plus a nonnegligible chemical energy (stored in the dissociated chemical species) at very high Mach numbers. Neglecting the thermal energy duplication of the asymptotic total enthalpy would imply $H_\infty = H_{\infty t}$ where

$$H_\infty = h_\infty + \frac{V_\infty^2}{2} \cong \frac{V_\infty^2}{2}$$
$$(H_\infty)_t = (c_p T_\infty)_t + (h_{ch\infty})_t + \frac{(V_\infty^2)_t}{2} \cong (h_{ch\infty})_t + \frac{(V_\infty^2)_t}{2} \tag{3}$$

The fact that a nonnegligible part of the energy appears as chemical energy $(h_{ch\infty})_t$ related to air composition at the nozzle exit

Received 26 July 2006; revision received 3 October 2006; accepted for publication 3 October 2006.

*Full Professor, Department of Space Science and Engineering, Piazzale Tecchio 80; monti@unina.it. Senior Member AIAA.

†Associate Professor, Department of Space Science and Engineering, Piazzale Tecchio 80.

‡Ph.D. Student, Department of Space Science and Engineering, Piazzale Tecchio 80. Member AIAA.

substantially reduces velocity $(V_\infty)_t$ as compared with free-flight velocity (V_∞), as mentioned earlier.

In the presence of substantial dissociation (of molecular oxygen and nitrogen) the problem of simulation for blunt bodies differs from that of sharp bodies due to the different role played by catalycity.

Numerical Model

The computations have been performed by computational fluid dynamics (CFD) code Fluent [5]. At the velocities considered in this work the level of flowfield ionization can be neglected. Therefore the Dunn–Kang 5-species (N2, O2, NO, N, O) reaction finite-rate air chemistry model is used [6]. The flow is assumed to be in thermal nonequilibrium, according to the two-temperature model of Park [7]. Vibrational relaxation is modeled using a Landau–Teller formulation, where relaxation times are obtained from Millikan and White assuming simple harmonic oscillators. The solver uses a modification of the Chapman–Enskog formula [8] to compute the diffusion coefficient using kinetic theory: viscosity and thermal conductivity are derived from the kinetic theory of gases [9] as functions of Lennard–Jones parameters [10].

Species boundary conditions on the wall are assigned according to solid surface behavior. For a fully catalytic wall, chemical reactions are catalyzed at an infinite rate of reactions and mass fractions are equal to their local equilibrium value. This condition, which is a long way from reality, particularly for a sharp body, has been chosen to point out the investigated phenomena. For a noncatalytic wall, defined as a surface where no recombination occurs, the diffusive flux of atoms at the wall is set to zero. For surface temperature computation radiative equilibrium condition at the wall has been considered with an emissivity value of 0.8.

Code accuracy has been checked with a high enthalpy hyperboloid flare numerical benchmark [11]. Satisfactory agreement has been found with experimental and other numerical code results in terms of pressure and skin friction coefficients. Furthermore, satisfactory agreement has been found with an experimental test on the heat flux probe of the SCIROCCO facility [4].

All computations have been performed for sphere–cone geometry (joined at about 75 deg of the sphere azimuth angle). To underline the difference between the aerothermodynamic behavior of a sharp and a blunt body a sphere–cone configuration has been considered with a radius of 1 cm and 30 cm, respectively, with a semi-apex angle of the cone of 15 deg in both cases. Figure 1 shows the computational grids.

Results and Discussion

All the chosen points along a reentry trajectory (see Table 1) exhibit a maximum heat flux at the stagnation point of 3.5 MW/m^2 and correspond to a local radiation equilibrium temperature of about 2700°C. This temperature may appear at the limit of the most advanced UHTC materials, however, if due consideration is given to the relatively high thermal conductivity and the extremely high temperature gradients at the tip [12], the temperature decreases to 2300/2400°C (which does appear to be compatible with this class of materials [9]).

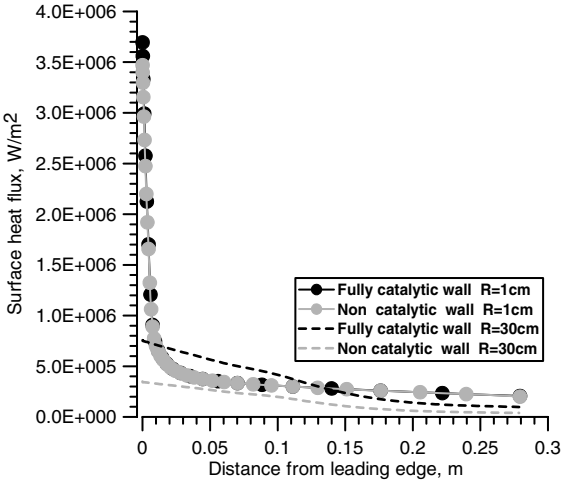

Fig. 2 Case 2: radiative equilibrium heat flux.

Figure 2 shows the difference between heat flux distribution for sharp and blunt bodies at local radiative equilibrium under the assumption of fully catalytic and noncatalytic wall (case 2 in Table 2, $Z = 70$ km, $M = 20.1$).

For a blunt body the bow shock detaches from the nose and dissociation reactions take place in the shock layer: a substantial difference on the surface heat flux in the two cases of fully and noncatalytic wall conditions exists.

With a sharp body chemical reactions take place only in a thin shock layer that surrounds the (small) leading edge: only near the stagnation point is there a nonnegligible difference between catalytic and noncatalytic wall.

For the thin shock layer of the sharp leading edge characteristic flow time (i.e., residence time between shock and nose) is smaller than the time necessary for the species to chemically equilibrate and air behaves as a frozen gas mixture. As a consequence it is possible to analyze heat transfer over a sharp body, in free flight, neglecting chemical reactions and assuming the perfect gas model.

Catalytic behavior of the surface material does not make any appreciable difference for sharp bodies. Indeed, one might expect a substantial difference between a fully catalytic and noncatalytic wall only if a nonnegligible percentage of total enthalpy in the shock layer is stored as dissociation energy, as is the case of the blunt body.

Table 2 shows stagnation point heat fluxes at the three points of the trajectory considered, for sharp body, respectively, for fully catalytic and noncatalytic wall. A difference exists at lower altitudes

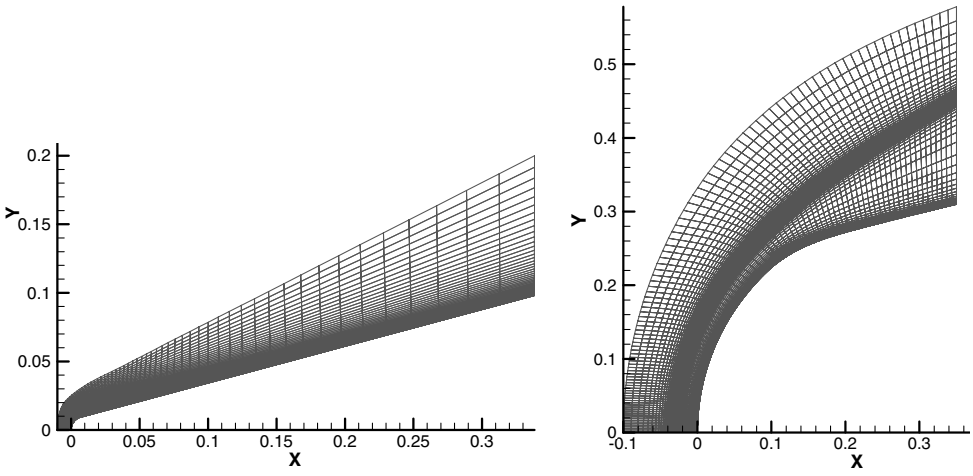

Fig. 1 Sharp and blunt nose computational grids.

Table 1 Free stream conditions corresponding to a $q_0 \approx 3.5$ MW/m^2 and $T_{ew} \approx 3000$ K for $R_n = 1$ [cm]

Case	Z, km	M_∞	V_∞, m/s	ρ_∞, kg/m^3	T_∞, K	Re_1
1	60	15.5	4909	3.1×10^{-4}	247	$1.9e+5$
2	70	20.1	5879	1.0×10^{-4}	210	$6.1e+4$
3	80	28.4	7400	2.1×10^{-5}	165	$1.4e+4$

Table 2 Stagnation point heat flux in free-flight condition (sharp body, $R_n = 1$ cm)

Case	Catalytic heat flux q_{FC}, Mw/m^2	Noncatalytic heat flux q_{NC}, Mw/m^2
1	3.25	2.8
2	3.7	3.5
3	3.3	3.3

($Z = 60$ km) where the dissociation that takes place in the shock layer is not negligible.

At first sight it may appear surprising that the dissociation effect is negligible at higher altitude and Mach numbers because of the higher temperature and lower pressure in the shock layer, conditions that favor dissociation. This is certainly true if we consider the chemical equilibrium condition. If we deal with highly nonequilibrium processes then the lower the pressure, the larger the chemical dissociation time so that frozen conditions tend to prevail.

A preliminary analysis based on nozzle flow CFD computations of different points of the operative envelope of the SCIROCCO PWT [4] has been carried out to identify the possible wind tunnel conditions capable of reproducing, in principle, the free-flight stagnation point heat flux. Table 3 shows the chosen conditions at the nozzle exit obtained from nozzle simulation.

All the simulations performed on sphere–cone geometries show that different behavior occurs between the cases of a noncatalytic and fully catalytic wall. To show this point let us assume that the wind tunnel is capable of supplying an air stream at the very same values of free flight:

$$(H_\infty)_t = H_\infty, \qquad (p_{02})_t = p_{02}$$

The Zoby engineering formula would then predict

$$(\dot{q}_0)_t = \dot{q}_0$$

However this is not true because a large part of the energy is stored in the dissociation energy in the tunnel air stream, which turns out to be chemically frozen immediately after the throat in all computed conditions and so, at the exit of the nozzle, there is a large amount of chemical enthalpy.

As a result if testing a noncatalytic sharp body in a wind tunnel, and if duplicating the free-flight values of H_∞ and p_{02}, a lower heat flux is obtained because the chemical part of the stream energy does not participate in energy exchange between the air and body surface.

Roughly, at very high Mach numbers, kinetic energy of the air stream in the wind tunnel is, neglecting the sensible enthalpy,

$$\frac{(V_\infty^2)_t}{2} \approx \frac{V_\infty^2}{2} - (h_{ch\infty})_t \tag{4}$$

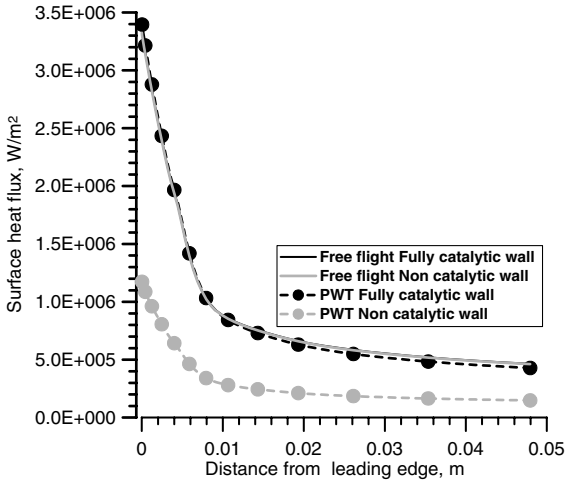

Fig. 3 Sharp body free flight (80 km) and PWT case B.

Therefore in a very first approximation heat flux would correspond to free-flight conditions with a reduced velocity $(V_\infty)_t$. Conversely, if the body surface is fully catalytic then one would expect the same heat flux in the wind tunnel and in free flight.

Figure 3 shows the numerical results obtained for free-flight conditions corresponding to altitudes of 80 km (see Table 1).

Figures 3 shows that free-flight heat flux (black and gray solid curves are coincident), which is not affected by the catalytic effect, can be well reproduced in the PWT only when the surface is fully catalytic (black curves). If a diffusion-limited approach is employed for a fully catalytic sharp body where the chemical processes are strongly diffusion limited, the results both in free-flight and PWT conditions could be in better accordance with those obtained with the noncatalytic wall results. As expected heat flux is substantially lower in the PWT test for a noncatalytic wall (gray curves).

An increase in total enthalpy leads to an increase in chemical dissociation, with more atomic species present at the exit of the nozzle and a higher percentage of chemical enthalpy (Fig. 4). As mentioned above this chemical enthalpy has no role to play in the surface heat transfer to the body in the case of a noncatalytic wall.

As a consequence, Table 4 shows that as total enthalpy of the flow increases the difference between fully catalytic wall and noncatalytic wall increases.

Things change when a blunt body is considered. In free flight the air passing through the bow shock, standing at a rather large distance in front of the body nose, has time to dissociate so that the heat flux for a catalytic or a noncatalytic wall can be very different.

Figure 5 illustrates the numerical results for case C; if the same blunt body is tested in a wind tunnel there is no great difference between the (large) heat flux for catalytic surface with respect to the free flight. There is no great difference for a noncatalytic wall either as the percentage chemical enthalpy in free flight and in PWT is almost the same.

So far the case in which both H_∞ and p_{02} can be reproduced in the tunnel has been considered.

As a rule $[(p_{02})_t/p_{02}] < 1$, and stagnation heat flux may be reproduced by setting $[(H_\infty)_t/H_\infty] > 1$ [equal to $\sqrt{p_{02}/(p_{02})_t}$]. At these conditions the wind tunnel stream exhibits larger degrees of dissociation and the differences between catalytic and noncatalytic

Table 3 PWT conditions in the test chamber

							Mass fractions			
Case	H_0, MJ/kg	p_t, Pa	M_t	V_t, m/s	T_t, K	ρ_t, kg/m^3	N_2	O_2	N	O
A	35	2.8	14.05	5202	173	3.2×10^{-5}	0.256	0	0.511	0.232
B	27	4.1	12	4981	250	3.5×10^{-5}	0.392	0.001	0.352	0.208
C	17	57	7.50	4471	670	2.3×10^{-4}	0.640	0.006	0.098	0.194
D	12	92	7.11	4030	678	4.0×10^{-4}	0.722	0.002	0.011	0.172
E	11	155	6.88	3960	729	6.5×10^{-4}	0.732	0.054	0.002	0.144
F	10	210	6.05	3848	800	8.2×10^{-4}	0.732	0.081	0	0.115

Table 4 Stagnation point heat flux in the PWT condition on sharp body

Case	H_0, MJ/kg	Catalytic heat flux q_{FC}, Mw/m^2	Noncatalytic heat flux q_{NC}, Mw/m^2
E	11	3.3	2.4
C	17	3.6	1.9
B	27	3.7	1.2

and between free flight and wind tunnel are greater; an accurate description and computation of the catalytic phenomena is mandatory in these cases.

Choosing high values of $(p_{02})_t$ and low values of $(H_\infty)_t$ (not an easy condition to obtain in arc–jet facilities) dissociation could be reduced, and the difference between free-flight and wind tunnel simulation would be smaller. Figure 6 shows how, for the same product $H_0\sqrt{p_{02}}$ and with the fully catalytic wall, heat flux values and distributions very similar to free-flight conditions may be obtained.

Figure 7 shows large differences between PWT and free flight reproducing the product $H_0\sqrt{p_{02}}$ with a noncatalytic wall.

In both cases PWT simulation is close to free-flight conditions for higher total pressure, that is, higher stagnation pressure and lower chemical enthalpy.

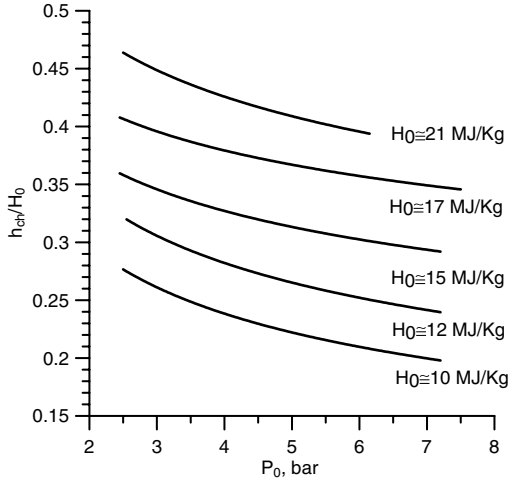

Fig. 4 Chemical–total enthalpy ratio versus total pressure at PWT inlet for different H_0.

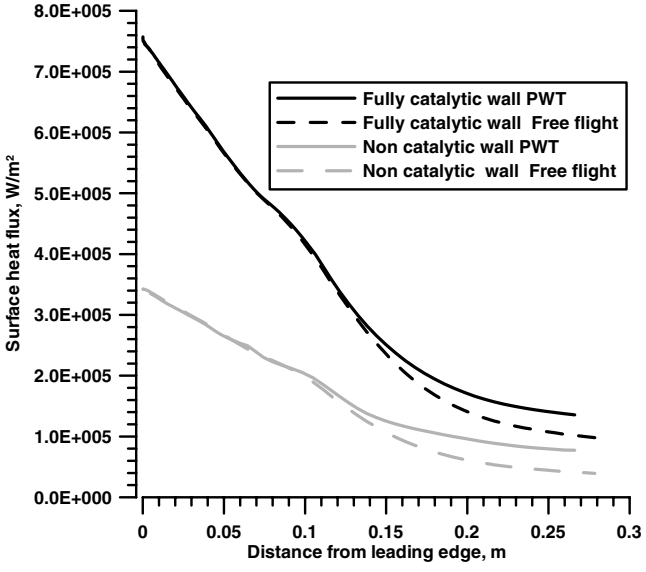

Fig. 5 Blunt body free flight (case 2) and PWT (case C).

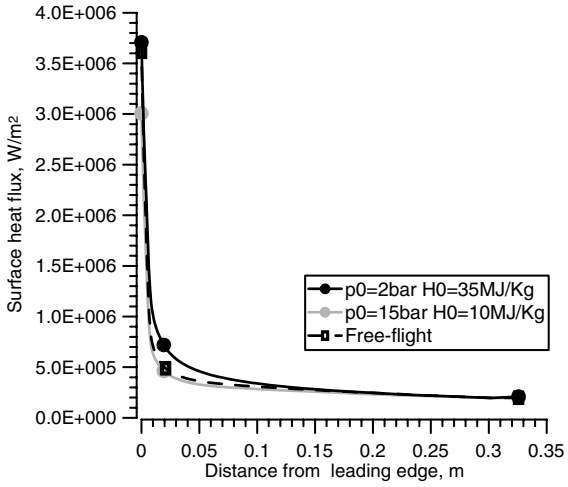

Fig. 6 Sharp body free flight (70 km) and PWT condition cases A and F; fully catalytic wall.

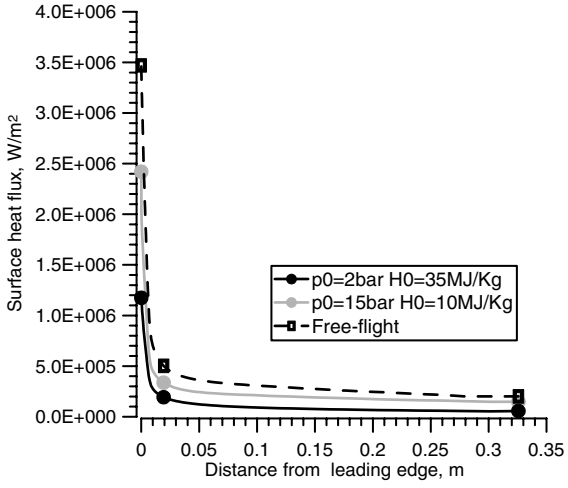

Fig. 7 Sharp body free flight (70 km) and PWT condition cases A and F; noncatalytic wall.

This difference is larger at higher total enthalpy of the flow (and lower total pressure).

These results point to the possibility of duplicating heat fluxes for catalytic and for blunt bodies in PWT; at the same time, they indicate the difficulty of the duplication of stagnation point noncatalytic heat flux for a sharp body reentering the atmosphere (in the case of diffusion-limited phenomena the fully catalytic heat flux is also difficult to duplicate). In particular, there is no tunnel setting for SCIROCCO capable of duplicating the same heat flux of the free flight for a sharp body reentering the atmosphere. This last consideration is the most important conclusion as regards PWT simulation for sharp bodies at the same scale and at the same wall material.

Conclusions

In free-flight blunt bodies exhibit a heat flux that, in the most severe reentry conditions, may amount to 50% higher for a fully catalytic wall than for a noncatalytic wall. Conversely, sharp bodies behave differently from blunt bodies when catalytic effects are taken into account: typically in free flight stagnation point heat flux for a sharp body is not greatly different (say about 10%) between a fully catalytic and a noncatalytic wall.

When simulating the aerothermochemistry in a plasma wind tunnel of arc–jet type the catalytic characteristics of the wall are much more important than for free-flight conditions for both sharp and

blunt bodies because of the large dissociation degree of both O_2 and N_2 in the test chamber airflow (which results from freezing of the composition in the nozzle). PWT testing at the same values of H_∞ and p_{02} may yield values of stagnation point heat transfer for a fully catalytic wall that may be 3 times larger than values for a noncatalytic wall. Thus, catalytic behavior is a relevant issue in PWT tests, as shown by CFD cases.

The third conclusion refers to the duplication of free-flight conditions in PWT with the same materials of free flight, (i.e., the same surface catalytic properties) at the same scale. It is simpler to simulate blunt bodies than sharp bodies. In the first case conditions in the shock layer are not expected to be dramatically different between free flight and PWT at the same H_∞ and p_{02}. For fully catalytic sharp bodies duplication of the above parameters corresponds to the same heat fluxes. A dramatic difference does exist, however, when simulating a sharp noncatalytic body reentry because of the difficulty of reaching high values of $(V_\infty)_t$ in the tunnel: when trying to increase the energy content of the air stream above a certain value (say $H_\infty \approx 20$ MJ/kg) by inputting more energy per unit mass, the surplus goes into dissociation energy that does not participate in the heat transfer to noncatalytic walls. The only choice is to have higher pressures rather than a larger H_0.

Acknowledgments

This work has been carried out with the partial support of the Italian Aerospace Research Centre and the Italian Space Agency.

References

[1] Monti, R., and Paterna, D., "Low Risk Reentry: Looking Backward to Step Forward," AIAA Paper 2005-3365, 2005

[2] Arnold, J., Johnson, S., and Wercinski, P., "SHARP: NASA's Research and Development Activities in Ultra High Temperature Ceramic Nose Caps and Leading Edges for Future Space Transportation Vehicles," International Astronautical Federation Paper IAF-01-V5-02, 2001.

[3] Zoby, E. V., "Empirical Stagnation-Point Heat Transfer Relation in Several Gas Mixtures at High Enthalpy Levels," NASA TN D-4799, 1968.

[4] De Filippis, F., Savino, R., and Martucci, A., "Numerical–Experimental Correlation of Stagnation Point Heat Flux in High Enthalpy Hypersonic Wind Tunnel," AIAA Paper 2005-3277, 2005.

[5] Anon., *Fluent 6.2 User's Guide*, Fluent Inc., Lebanon, NH, 2004.

[6] Park, C., "Review of Chemical Kinetics Problems for Future NASA Mission, Part 1: Earth Entries," *Journal of Thermophysics and Heat Transfer*, Vol. 7, No. 3, 1993, pp. 385–398.

[7] Park, C., *Nonequilibrium Hypersonic Aerothermodynamics*, Wiley, New York, 1990.

[8] McGee, H. A., *Molecular Engineering*, McGraw–Hill, New York, 1991.

[9] Hirscfelder, J. O., Curtiss, C. F., and Bird, R. B., *Molecular Theory of Gases and Liquids*, Wiley, New York, 1954, pp. 75–106.

[10] Anderson, J. D., Jr., *Hypersonic and High Temperature Gas Dynamics*, McGraw–Hill, New York, 1989.

[11] Grasso, F., Marini, M., and Morinischi, K., *First Eastern Western High Speed Flow Field Database Workshop*, Kioto Institute Of Technology, Kioto, 1998, pp. 1–48.

[12] Monti, R., De Stefano Fumo, M., and Savino, R., "Thermal Shielding of Reentry Vehicle by UHTC Materials," *Journal of Thermophysics and Heat Transfer*, Vol. 20, No. 3, pp. 500–506, 2006.